# A new mix design method for low-environmental-impact blended cementitious materials: Optimization of the physical characteristics of powders for better rheological and mechanical properties

Oumayma Ahmadah, Hela Bessaies-Bey, Ammar Yahia, Nicolas Roussel

# A new mix design method for low-environmental-impact blended cementitious materials: Optimization of the physical characteristics of powders for better rheological and mechanical properties

Oumayma Ahmadah*[a,b,c], Hela Bessaies-Bey[a], Ammar Yahia[b], and Nicolas Roussel[c]

[a]CPDM, IFSTTAR, Université Gustave Eiffel, Champs-sur-Marne, France
[b]Université de Sherbrooke, Department of Civil and Building Engineering, Sherbrooke, Québec, Canada
[c]Laboratoire Navier, IFSTTAR / CNRS / ENPC, Université Gustave Eiffel, Champs-sur-Marne, France

*Corresponding author: Oumayma.ahmadah@usherbrooke.ca

## Abstract

The use of blended cements has attracted much interest in the quest to overcome the environmental challenges facing the concrete industry. However, partially replacing cement with supplementary cementitious materials (SCMs) can result in complex rheological behavior that is influenced by the type of SCM and the replacement percentage, as well as the physical characteristics of the particles. Adequate physical control of the blended cements is essential for improving the rheology of the suspensions. A new mix design methodology based on the physical optimization of SCMs is proposed and validated to ensure adequate rheology of the suspensions. The physical characteristics that influence the viscosity of the cement-based suspensions investigated in this study include particle-size distribution, surface roughness, maximum packing density of the powder, and interparticle distance. Based on the experimental results presented in this paper, ternary binders with optimized physical characteristics enhanced the 28-day compressive strength of mortar by 20% while decreasing the clinker content by 15% and maintaining constant fluidity.

**Keywords:** Supplementary cementitious materials; Physical characteristics; High-range water-reducer; Rheology; Compressive strength; Optimization.

# 1. Introduction

Supplementary cementitious materials (SCMs) are commonly used to partially replace cement to reduce the environmental impact of cement-based materials. Using supplementary cementitious materials modifies the physical characteristics of the cement-based materials, including the specific surface area (SSA), the packing density, and the shape of particles in blended systems [1-6]. These properties significantly influence the workability of concrete [4,5] [7-14]. It is reported that the increase in mean diameter ($d_{50}$), dry packing density, circularity, coefficient of uniformity ($C_u$), and $d_{50}^2$/SSA ratio resulted in higher flowability in the blended systems, which reflects lower plastic viscosity and yield stress values [15,16]. However, the existing predictive models only consider a few of the parameters that influence viscosity and yield stress. Optimizing the physical characteristics of powders to ensure adequate rheological properties is therefore based on a trial-and-error approach rather than a scientific approach. This is time consuming and may result in the concrete having inadequate rheological properties due to uncontrolled variations in particles' physical properties.

In addition to the SCM's physical characteristics, incorporating a high-range water-reducer (HRWR) influences the rheological behavior of concrete by decreasing its yield stress and plastic viscosity [14] [17-20]. HRWRs, especially PCEs, which are known to be the most efficient plasticizers [21], increase the interparticle distance through steric hindrance. This reduces the attractive forces [22-23], decreasing the yield stress and the plastic viscosity of the suspension [20]. However, although they induce extra cost, it has been proven that these chemical admixtures are more efficient in decreasing the yield stress than the plastic viscosity [20]. This can result in "sticky" concretes that are hard to vibrate and surface finish. Furthermore, the new generation of cement has finer particles, mostly due to its silica fume content, which increases the need for a HRWR [24]. Controlling the rheological parameters of cement-based suspensions will thus not be possible if the compatibility of SCMs with HRWRs is the only consideration; optimizing the physical characteristics of SCMs to ensure adequate rheology of suspensions will also be necessary. Investigating the effect cementitious materials' physical characteristics have on the rheology of the suspension makes it possible to go beyond simply understanding their influence on the yield stress and

plastic viscosity variations. Indeed, it can facilitate the approach to selecting powders with adapted physical characteristics to ensure proper rheology, while targeting materials with enhanced mechanical behaviors.

Different approaches to optimize the physical characteristics of powders for better workability and better mechanical properties were reported in the literature [6,25]. In [25], the authors focused on enhancing the rheological behavior of the suspension by optimizing the maximum packing density of the powders. However, the rheology of cementitious suspensions also depends on other physical characteristics of particles such as their size. In [6], the authors proposed a numerical approach for evaluating density, the mean centroidal distance, and the coordination number of the microstructure in order to optimize blended cements.

The main objective of this investigation is to develop an approach to optimize the physical characteristics of binders and to proportion blended cement-based suspensions with an adapted rheology (lowest plastic viscosity and yield stress) and improved mechanical properties. As seen in Table 1, the key physical parameters of cementitious powders (i.e. particle size, roughness, and packing density) have a contradictory effect on the rheological and hardened properties of cement-based materials. Consequently, selecting powders with optimal physical characteristics is challenging, and the details of the physical correlations between all the key parameters (i.e. particle size, roughness, and maximum packing) should be taken into consideration. Moreover, the physical characterization of blended cements can be complicated and time consuming, specifically in the case of blended powders with variable physical properties and size. The approach proposed in the first part of this study aims to use models such as the compressible packing model (CPM) to predict the physical characteristics of blended cements relying on the physical characterization of single powders [26]. The physical characteristics of the blended cements are then incorporated in predictive models to quantify the plastic viscosity and yield stress of the corresponding suspensions. That enables us to select SCMs to formulate a binder with the necessary physical characteristics in order to give the cement-based material the best possible rheological and mechanical behavior. The models used to predict the yield stress and the viscosity were previously validated on unblended as well as blended cementitious powders with SCMs (clinker, slag, limestone, quartz, and fly ash) [27]. In this paper, these models will be applied

to a ternary cement compound of 65% clinker, 20% slag, and 15% limestone filler. This cement is a low-carbon-footprint ternary cement called CEM II/B-M (S-LL), which is named according to European standards. Different ternary binders were made with the same proportions of SCMs (slag and limestone). Slag and limestone filler powders with different physical characteristics were used to vary the physical characteristics of the blended systems. The chemical composition of the single powders of the investigated slag and limestone fillers were controlled when evaluating the effect of the physical optimization on the mechanical strength of the hardened mortar.

Based on the results, the compressible packing model (CPM) [26] adequately predicted the packing density of blended cements using the physical properties of the single powders. On the other hand, the existing viscosity and yield stress models [14,27] accurately estimated the rheological properties of blended cement suspensions by measuring the physical properties of the blended cements. The proposed approach makes it possible to physically optimize the binders, which enables the improvement of the mechanical properties of relatively concentrated suspensions while maintaining their fluidity.

## 2. Yield stress and plastic viscosity models: Scientific background

The rheological behavior of blended cement suspensions can be controlled by mean of their plastic viscosity and yield stress. The yield stress depends on the attractive forces between particles, the physical characteristics of the powders, and the solid fraction of the suspension [14,17]. The Yodel [14,17] can be used to estimate the yield stress of cement-based suspensions given the solid fraction and the maximum packing density of the powders. The Yodel is given in Eq. 1.

$$\tau_0 = m_1 \frac{\phi(\phi-\phi_0)^2}{\phi_{max}\,(\phi_{max}-\phi)} \qquad (1)$$

where $\tau_0$ is the yield stress, $\phi$ and $\phi_{max}\ are$ the solid volume fraction and maximum packing density of the powder, respectively, $\phi_0$ is the solid fraction of percolation, and $m_1$ is a correlation factor that that takes into account interparticle forces, size of particles, radius of curvature at the contact points, and the powders' particle distribution. The parameter $m_1$ is defined in Eq. 2, as follows:

$$m_1 = \frac{1.8}{\pi^4} G_{max} a^* u_{k,k} \left(\frac{f^*_{\sigma,\Delta}}{R^2_{v,50}}\right) \quad (2)$$

where $a^*$ is the mean radius of curvature at contact points, $R_{v,50}$ is the volume mean radius, and $G_{max}$ is the maximum interparticle force. In this paper, we refer to $a^*$ by the particle's roughness. On the other hand, the $G_{max}$ is defined by the Eq. 3, as follows:

$$G_{max} = \frac{A_0}{12h^2} \quad (3)$$

where $A_0$ is the Hamaker constant, $h$ is the interparticle distance, and $f^*_{\sigma,\Delta}$ describes the particle-size distribution of the powder, which is defined in Eq. 4, as follows:

$$f^*_{\sigma,\Delta} = \frac{1}{u_{k,k}} \sum_{k=1}^{m} \phi_k \sum_{l=1}^{m} S_{a,l} \frac{A_s}{A_c} \frac{\Delta v_{k,l}}{b_k^3} \frac{1}{(b_k^2 + b_l^2)} \quad (4)$$

where $b_i$ is the particle radius ($a_i$) normalized by the volume-average radius $R_{v,50}$ and $\phi_k$ is the volume fraction of particles of size $b_k$ in the size range k. $A_s/A_c$ and $S_{a,l}$ are geometrical parameters for the coordination number of a packed bed of size-distributed spheres, $\Delta v_{k,l}$ is a geometrical term that accounts for a change in the maximum packing fraction induced by each pair of undispersed particles of sizes $a_k$ and $a_l$, $while\ u_{k,k}$ is a normalization factor that makes $f^*_{\sigma,\Delta}$ unity for monodispersed systems. They are defined by Eqs. 5 - 8, as follows:

$$\frac{A_s}{A_c} = \frac{2(b_l + b_k)}{b_k + b_l\sqrt{b_k(b_k + 2b_l)}} \quad (5)$$

$$S_{a,l} = \frac{\phi_l / b_l}{\sum_{i=l}^{m} \phi_i / b_i} \quad (6)$$

$$\Delta v_{k,l} = 4\pi(b_k b_l)(b_k + b_l) \quad (7)$$

$$u_{k,k} = \frac{16\pi}{2 - \sqrt{3}} \quad (8)$$

A model linking the plastic viscosity of cementitious suspensions to the physical characteristics of powders was also proposed [27]. This model accurately predicted the viscosity of both single powder-based and blended powder-based suspensions. The model is given in Eq. 9, as follows:

$$\mu = 0.16\mu_0 \frac{a^{*2}}{h d_{50}} \left(1 - \frac{\phi}{\phi_{max}}\right)^{-3} \quad (9)$$

where $\mu_0$ is the viscosity of the suspending phase, $a^*$ is the mean radius of curvature at contact points, $d_{50}$ is the volume mean diameter, $h$ is the interparticle distance, while $\phi$ and $\phi_{max}$ are the solid volume fraction and maximum packing density of the powder, respectively.

For a given blend composition and solid volume fraction, the effect of the physical characteristics of a powder on the rheological and mechanical properties of a cement-based suspension can be identified, as shown in Table 1. It was assumed that the specific surface area increases with the particles' roughness. This means that increasing the roughness has the same effect of decreasing the particles size (or increasing the specific surface area) on both the rheological and mechanical properties. In general, for cementitious powders, including Portland cement, slag, and limestone filler, the roughness of particles does not change much [27]. It is reported that the roughness is of the order of few hundreds of nanometers [27]. In the case of strongly flocculated cementitious suspensions (i.e. without HRWR), the interparticle distance is constant and is of the order of few nanometers [27, 28]. On the other hand, for concentrated suspensions, the percolation fraction does not affect significantly the yield stress [14]. An average value of 20% for the percolation fraction is reported in literature [26-27]. Thus, the particles size and the maximum packing density are the mean physical parameters that influence the rheological and mechanical performance of cementitious suspensions.

**Table 1. Expected dependencies of the rheological and mechanical properties of cement paste mixtures to the physical properties of powders**

| Physical parameters variation | Plastic viscosity | Yield stress | Early mechanical strength | 28-D Mechanical strength |
|---|---|---|---|---|
| **Increase in the particle's size** | Decreases [27] [9] [10] | Decreases [14] [35] | Decreases [31,32,33] | Low effect (decrease with the solid fraction) [33,34] |
| **Increase in the maximum packing density** | Decreases [27] | Decreases [14] | (Unknown, based on the author's knowledge) | Low effect [33,34] May enhance the pozzolanic reaction [36] |
| **Increase in the particle's roughness** | Increases [27] | Increases [14] | (Unknown, based on the author's knowledge) | Low effect |

# 3. Materials and protocols

## 3.1. Materials

The powders investigated in this study include a Portland cement, three limestone fillers (Limestone 4, Limestone 10, and Limestone 11.5), and three slag powders (slag 5.5, slag 6.5, and slag 11.5). The chemical composition and Bogue composition of the Portland cement are summarized in Table 2. The density of these powders was determined using the wet pycnometer method [37]. In addition to these powders, slag 6.5 and limestone 11.5 were softly ground for 30 minutes using a Los Angeles type ball mill to obtain slag 5 and limestone 4.5, respectively. The grinding procedure was carefully selected to avoid a temperature rise during grinding. This was done to obtain powders with different physical characteristics (i.e. particle size and packing density) while keeping a similar chemical composition. This allows for the evaluation of the sole effect of physical optimization on the mechanical strength of mortars. The volume mean diameter, maximum packing density, and the density of the investigated powders are presented in Table 3. A standard sand with a density of 2650 kg/m$^3$ and a maximum packing density of 66% (using an intensive compaction tester [38]) was used in mortar mixtures.

***Table 2. Chemical and Bogue composition of the Portland cement***

| **Chemical composition** | **(%)** | **Bogue mineralogical composition** | **(%)** |
|---|---|---|---|
| **CaO** | | **$C_3S$** | 63 |
| **63.8** | | **$C_2S$** | 9.8 |
| **$SiO_2$** | | **$C_3A$** | 7.1 |
| **20** | | **$C_4AF$** | 8.1 |
| **$AL_2O_3$** | | | |
| **4.4** | | | |
| **MgO** | | | |
| **2.0** | | | |
| **$SO_3$** | | | |
| **3.6** | | | |
| **$Fe_2O_3$** | | | |
| **2.6** | | | |
| **$NA_2O$** | | | |
| **0.78** | | | |
| **Cl-** | | | |

| | | |
|---|---|---|
| **0.003** | | |
| **Insoluble residue** | **0.4** | |
| **Loss on ignition** | **2.5** | |

*Table 3. Volume mean diameter, maximum packing density, and density of the investigated powders*

| Materials | Volume mean diameter (µm) (Section 3.2) | Maximum packing density (%) (Section 3.3) | Density (Kg/m$^3$) |
|---|---|---|---|
| **Portland Cement (GUP)** | 6.3 | 56.6 | 3110 |
| **Limestone 4** | 3.9 | 56.5 | 2740 |
| **Limestone 10** | 10.2 | 56.8 | 2740 |
| **Limestone 11.5** | 11.4 | 64.5 | 2740 |
| **Limestone 4.5 ground from Limestone 11.5** | 4.6 | 59.5 | 2740 |
| **Slag 5.5** | 5.6 | 57.8 | 2930 |
| **Slag 6.5** | 6.5 | 56.3 | 2880 |
| **Slag 8.5** | 8.5 | 56.5 | 2900 |
| **Slag 5 ground from Slag 6.5** | 5.2 | 56.5 | 2880 |

## 3.2. Particle-size distribution

For each powder type, the particle size distribution was determined using the laser diffraction method in isopropanol. Before each measurement, the sample (powder and isopropanol) was deflocculated using ultrasound for 15 minutes. The obtained particle-size distribution curves of the Portland cement, slag, and limestone filler single powders are summarized in Figure 1 and Figure 2, respectively. The particle-size distributions of blended powders were estimated using the size distribution of the single powders and their volumetric fractions in the blended systems. The particle-size distribution characteristics of the blended powder are summarized in Table 4.

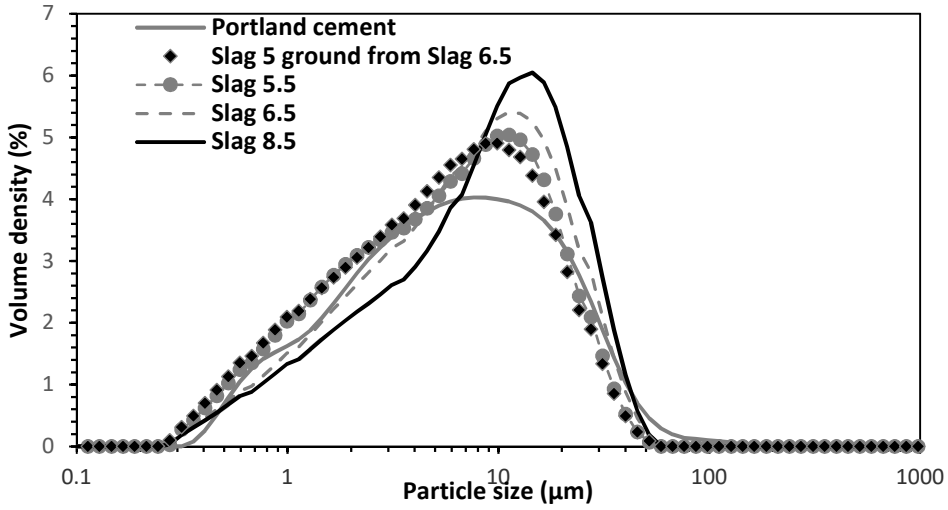


**Figure 1.Particle-size distributions of Portland cement and slag powders**

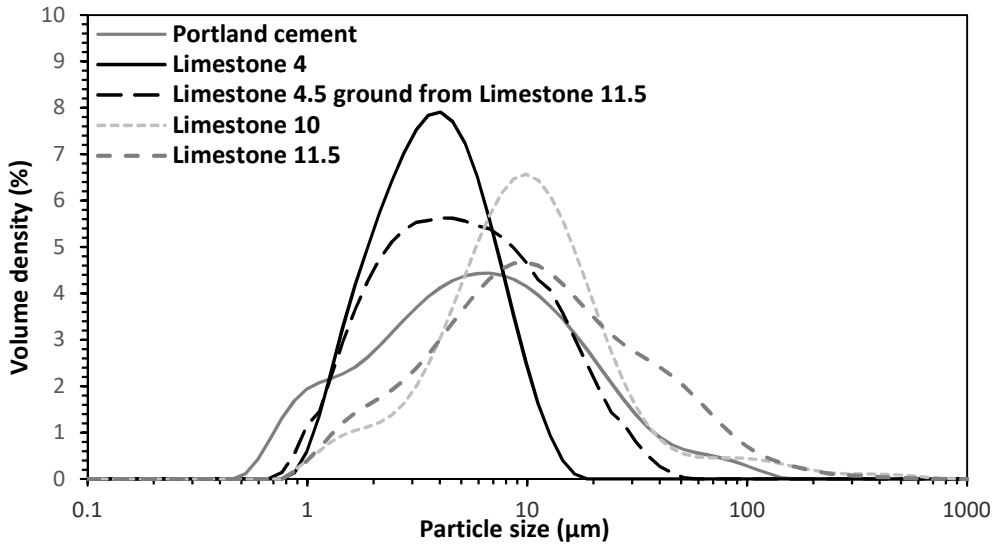


**Figure 2.Particle-size distributions of Portland cement and limestone powders**

## 3.3. Powder packing density measurements

The packing density measurements were performed using the test method developed by Sedran et al. [39]. This method consists in determining the minimum amount of water needed to obtain a homogeneous cement paste. The minimum amount of water corresponds to the quantity of water necessary to fill the available pore volume in the system. The method involves first mixing 350g of cement at low speed with a given quantity of water and an optimized amount of HRWR for one minute using a planetary mixer. The

optimum HRWR amount corresponds to its saturation dosage for which there is no further increase in the maximum packing density of the system. The water was gradually added each minute of mixing. When a homogeneous cement paste is obtained, the total amount of water added corresponds to the required amount to fill all the existing pores in the system. The maximum packing density is given by Eq. 10, as follows:

$$\phi_{max} = \frac{volume_{powder}}{volume_{powder} + volume_{water}} \quad (10)$$

## 3.4. Mixing sequence and sample preparation

Different ternary blended systems were proportioned using 65% Portland cement, 20% slag, and 15% limestone filler. The proportions are expressed by mass of the total binder content. We recall that for the same used SCM type, the densities of the powders are almost the same, which means that the volumetric proportion of each material in the blended system doesn't change while changing the powder for constant mass proportion. Furthermore, as mentioned earlier, the inert powders (four limestone fillers and four slag powders) were carefully selected to cover a wide range of physical properties of the blended cement and consequently quantify their effect on the rheological properties of suspensions. The powders were hand mixed using a spatula for two minutes before preparing the paste mixtures. The investigated cement mixtures were proportioned with a mass water-to-binder ratio (w/b) of 0.45 using a high-shear mixer. The mixing sequence involves subjecting the mixture to a high rotational shear of 10,000 rpm for two minutes. The mixture was then left to rest for one minute before carrying out the rheological measurements using a coaxial-cylinder rheometer.

The mortars were proportioned with a constant sand content of 1428 kg/m$^3$ and a superplasticizer dosage of 1.15 Kg/m$^3$. The mixing procedure was carried out according to ASTM C305 specifications [40]. All mortars were prepared in 1.8 L batches using a planetary mixer at two different speeds (140 rpm [$V_1$] and 285 rpm [$V_2$]). The mixing sequence involved mixing the water with the HRWR for a few seconds before introducing cement. The mixture was homogenized for one minute at low speed before introducing sand. The sand was then

introduced within 30 seconds, and two additional mixing sequences of one minute at low speed and 30 seconds at high speed were performed. The mixer was then stopped for 90 seconds to clean the walls of the bowl and verify the presence of agglomerated particles. Finally, mortars were mixed for another 60 seconds at high speed. A total mixing duration of five minutes was adopted to prepare the mortars.

## 3.5. Rheological measurements

In the case of cement paste mixtures, the apparent shear-viscosity measurements were carried out using a coaxial-cylinder rheometer with serrated surfaces. The diameters of the cup and bob are 28.911 mm and 26.660 mm, respectively, providing a shear gap size of 1.126 mm. The flow curves were determined after applying a pre-shear regime at 200 $s^{-1}$ for 120 s. The shear rate was then decreased in steps from 100 $s^{-1}$ to 1 $s^{-1}$ for 40 s to ensure a state of equilibrium at each shear rate. All the rheological measurements were conducted at a constant temperature of 24°C ±1°C. The flow curves of the investigated suspensions are described using the Bingham model, for which the apparent viscosity can be evaluated as follows: $\mu = \mu_{plastic} + \frac{\tau_0}{\dot{\gamma}}, where$ $\tau_0$ is the yield stress of the suspension and $\mu_{plastic}$ is the plastic viscosity.

The workability of mortar mixtures was assessed using a mini-cone test having upper and lower diameters of 70 mm and 100 mm, respectively, and a height of 60 mm. The yield stresses and viscosity values of the investigated mortar mixtures were then calculated using the Eqs. 11 and 12 [41, 42], respectively, as follows:

$$\mu_0 = \frac{0{,}0081}{2R^{3{,}649}} \quad (11)$$

$$\tau_0 = \frac{225\rho g \Omega^2}{128\pi^2 R^5} \quad (12)$$

where ρ is the density of the mixture, g is the gravity, $\Omega$ is the volume of the tested sample, and R is the radius of the spread diameter in the cone test.

## 3.6. Compressive strength measurements

For each mortar, the compressive strength of the investigated material was assessed by sampling various 50 $mm^3$ cubes. Immediately after casting, the samples were properly

covered to prevent evaporation and stored at ambient laboratory temperature for 24 hours. The samples were then removed from the mold and stored in a sealed plastic bag until the age of testing. The compressive strength measurements were carried out after seven days of age and 28 days of age according to the ASTM C 109 specifications. A constant loading rate of 2400 N/s was employed for all the mixtures.

# 4. Test results and discussions

The test results are presented in terms of the calculated physical properties of blended powders, the rheological properties of the investigated paste mixtures, and the compressive strength of the optimized mortars.

## 4.1. Packing density of blended powders: Validation of the CPM model

The investigated ternary blended systems as well as their calculated volume mean-diameter and measured packing density values are summarized in Table 4. In addition, the compressible packing model (CPM) [26] was used to estimate the theoretical packing density of blended powders. The CPM model [26] is expressed as follows:

$$\gamma = \inf(\gamma_i) \qquad (13)$$

$$\gamma_i = \frac{\beta_i}{1-\sum_{j=1}^{i-1}\left[1-\beta_i+b_{ij}\beta_i\left(1-{}^{1}/_{\beta_i}\right)\right]x_{vj}-\sum_{i+1}^{n}\left[1-a_{ij}{}^{\beta_i}/_{\beta_j}\right]x_{vj}} \qquad (14)$$

$$a_{ij} = \sqrt{(1-(1-d_j/d_i)^{1.02}} \qquad b_{ij} = 1-(1-d_j/d_i)^{1.5} \qquad (15)$$

$$K = \sum_{i=1}^{n} \frac{{}^{\gamma_i}/_{\beta_i}}{{}^{1}/_{C}-{}^{1}/_{\gamma_i}}$$

where y is the maximum packing density of the blended powder, $\beta_i$ is the maximum packing density of class i of the powder, $d_i$ is the volume average diameter of class i of the powder, and $x_{vi}$ is the volume proportion of class i of the powder. On the other hand, $a_{ij}$ et $b_{ij}$ functions describe the interactions between particles, C is the experimentally measured maximum packing density of a single powder, and K is the tightness index.

***Table 4. Measured volume mean diameter and maximum packing densities for the ternary investigated systems***

| Ternary systems (65% - 20% - 15%) | Calculated volume mean-diameter (μm) | Measured maximum packing density (%) |
|---|---|---|
| **Cement – Slag8.5 - Limestone4** | 5.75 | 56.5 |
| **Cement – Slag8.5 - Limestone10** | 6.7 | 57.5 |
| **Cement – Slag8.5 - Limestone11.5** | 6.9 | 57.3 |
| **Cement – Slag5.5 - Limestone4** | 5.2 | 57.8 |
| **Cement – Slag5.5 - Limestone10** | 6.1 | 57 |
| **Cement – Slag5.5 - Limestone11.5** | 6.3 | 57.2 |
| **Cement – Slag6.5 - Limestone4** | 5.35 | 56.8 |
| **Cement – Slag6.5 - Limestone10** | 6.3 | 56.4 |
| **Cement – Slag6.5 - Limestone11.5** | 6.47 | 57.0 |

The relationship between the calculated and experimental packing density values of the investigated ternary binder systems is shown in Figure 3. Our results show that it is not easy to predict if the maximum packing density of a blend will be higher or not in comparison to another blend based only on the maximum packing densities of each single powder as it is the case for Cement-Slag 8.5-Limestone 10 in comparison with Cement-Slag 8.5-Limestone 11.5 for instance. The CPM model allows indeed for an accurate maximum packing density estimates of the blended system based on both the particles size distribution and packing density of each powder in the binder as shown in Figure 3. The predicted packing density values are very close to the experimental values. This suggests that the physical characterization, including the particle-size distribution (PSD) and maximum packing density, of the blended systems can be accurately estimated using the proportion ratio as well as the physical characteristics of each single powder in the blended system. Accordingly, the maximum packing densities of ternary blended binders with constant chemical composition (i.e. using ground powders and the unground original materials) are calculated and summarized in Table 5.

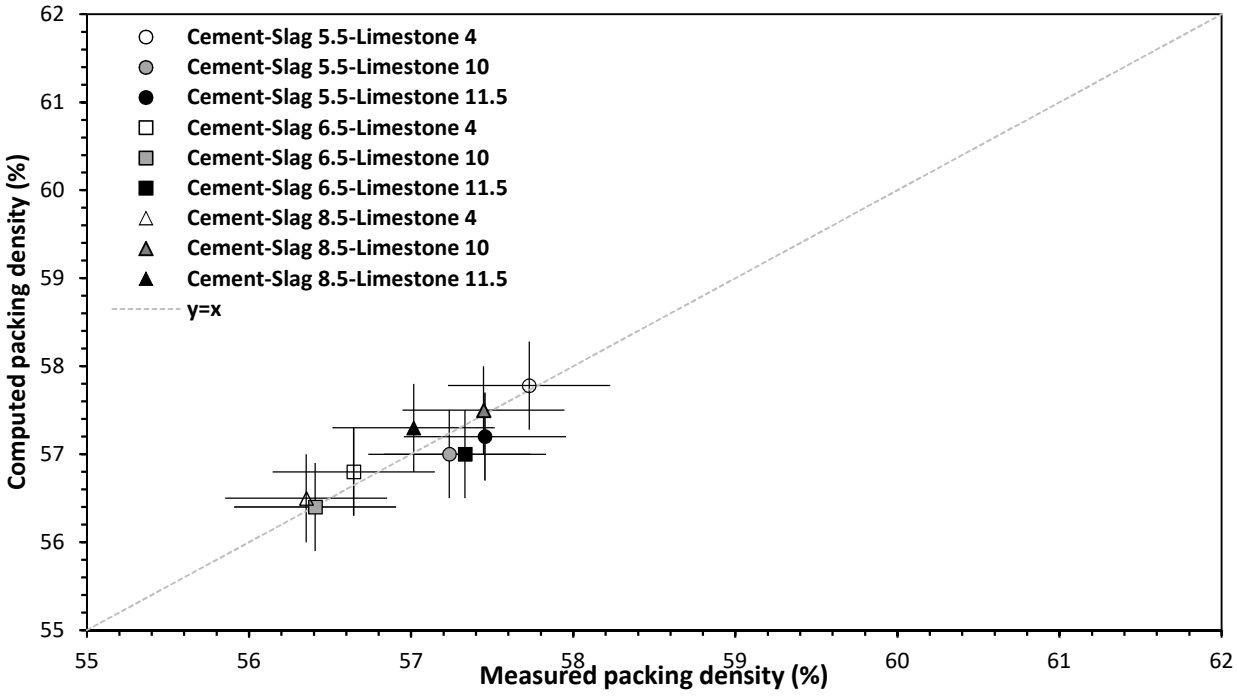


**Figure 3. Relationship between calculated and experimental packing density values of the investigated ternary binder systems**

**Table 5. Calculated volume means diameter and maximum packing densities of ternary blended cements**

| Ternary binders (65% - 20% - 15%) | Computed volume mean-diameter (µm) | Calculated packing density (%) |
|---|---|---|
| **Cement - Slag6.5 - Limestone11.5** | 6.47 | 57.3 |
| **Cement - Slag6.5 - Limestone4.5** | 5.4 | 57.7 |
| **Cement - Slag5 - Limestone11.5** | 6.2 | 58.3 |
| **Cement - Slag5 – Limestone 4.5** | 5.0 | 58.7 |

## 4.2. Prediction and optimization of the rheological properties of suspensions

The relationship between the measured and calculated rheological parameters (plastic viscosity and yield stress) of the investigated cement paste mixtures are presented in Figure 4. The calculated yield stress and plastic viscosity values for the 12 ternary blended cements were obtained using Eqs. (1) and (9), respectively. The calculated rheological parameters accurately estimated the experimental values, especially in the case of plastic viscosity. The observed variations of yield stress prediction may be due to the use of an average value of

the percolation fraction for the investigated blended powders. In fact, the percolation fraction of a powder may depend also on its maximum packing density [18]. However, the discrepancies are within an acceptable range of the error of measurement, which confirms the adequacy of the assumed hypothesis concerning the percolation fraction's weak impact on the yield stress of concentrated suspensions. As shown in Figure 4, the results confirm the adequacy of the viscosity model [27] and the Yodel [14,17] in predicting the rheological properties of blended cement suspensions using the physical characteristics of each single powder. In addition to allowing precise prediction of the cementitious suspensions' rheology given the physical characterstics, the models given in Eqs. 1 and 9 can be used to determine the composition of the ternary blended systems that result in a suspension with the lowest plastic viscosity and yield stress values according to the application at hand. Therefore, a basic characterization of the maximum packing density and size distribution of the single powders allowed the design of a ternary cement powder with characteristics that are optimized to achieve the targeted rheology. By comparing the upper and lower limits of the rheological parameters, we conclude that thanks to the physical optimization of the cement powders, we have been able to reduce the suspension's plastic viscosity by 30% and its yield stress by 50% compared to a realistic combination of a non-optimized physical properties, while keeping the same proportions of each powder in the blended cement.

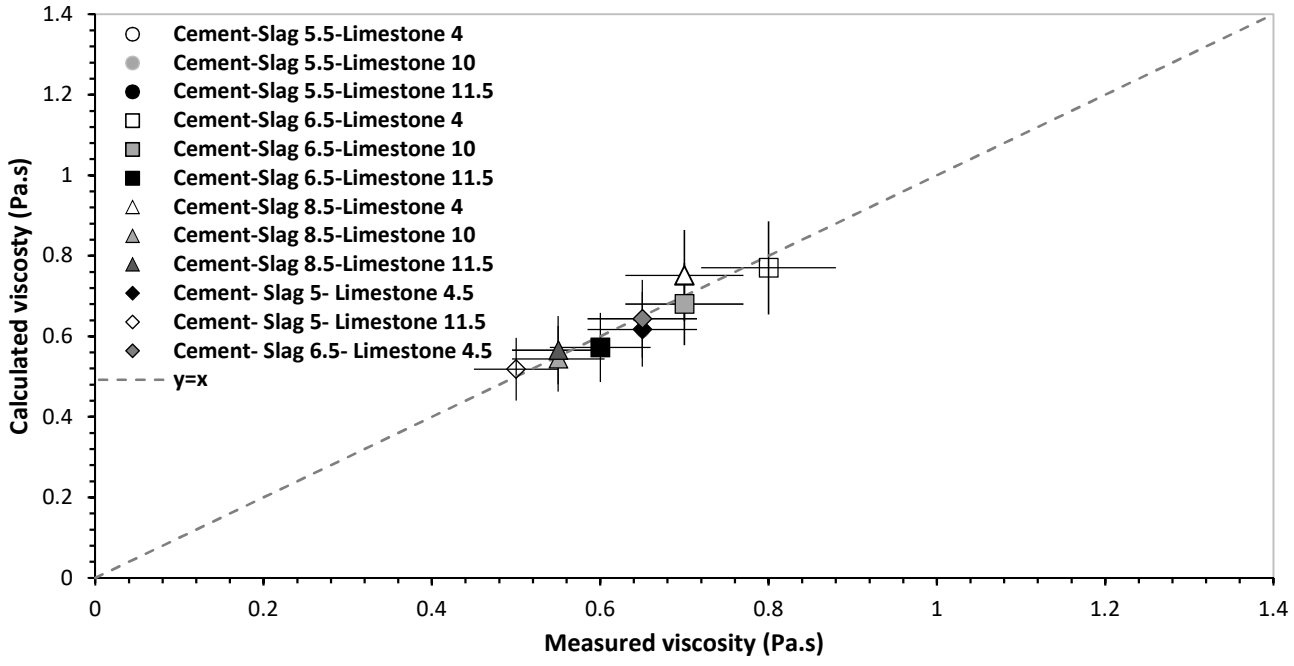

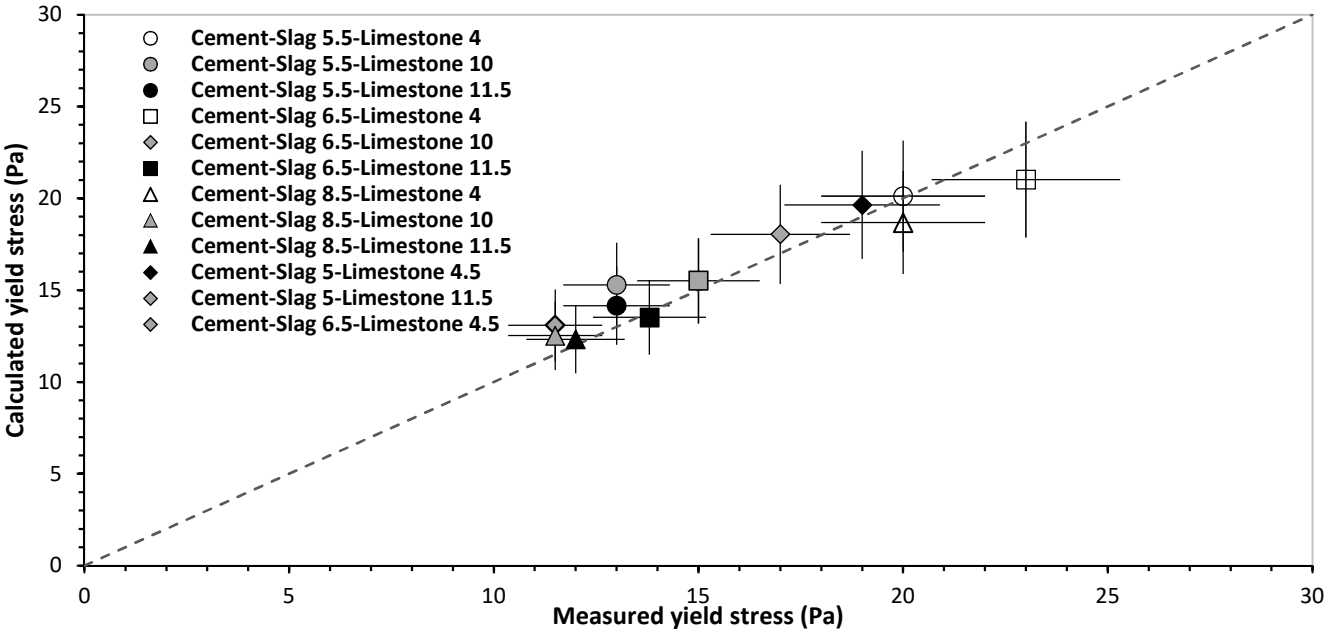


**Figure 4. Relationship between the calculated and measured plastic viscosity and yield stress of a cement-based suspension made with ternary blended systems (solid volume fraction = 42.5%)**

## 4.3. Optimization of mechanical properties

According to the reference blend composition (65% cement, 20% slag, and 15% limestone), four ternary binders with constant chemical compositions were proportioned to highlight the effect of physical optimization on the strength development of mortars. The physical characteristics of these blended cements were given in Table 5, using the physical characteristics and the proportion of each single powder in the blended system. As mentioned earlier, the grinding process was carried out to maintain the chemical composition of each single powder while changing its physical characteristics. It is assumed that the soft grinding does not change the reactivity of the system, which will be confirmed later in this paper. All the ternary binders have an equal density of 2970 kg/m$^3$. Another ternary binder made with a lower clinker content was also optimized using the same single powders (50% cement, 30% slag, and 20% limestone) to evaluate the effect of physical optimization on the mechanical strength of mortar with a lower clinker content. The average

particle size and maximum packing density values for this blended cement are six µm and 59.3%, respectively.

Among the investigated suspensions with a constant chemical composition shown in Figure 4, the ternary binder made with cement, slag 5, and limestone 11.5 exhibited the best rheological behavior, reflected by the lowest plastic viscosity and yield stress values. The binder made with cement, slag 5, and limestone 4.5 resulted in the highest viscosity and yield stress values. By comparing the upper and lower limits of the rheological parameters for suspensions with the same chemical composition, it can be concluded that the physical optimization of the powders reduced the plastic viscosity and yield stress of suspensions by 17% and 35%, respectively, compared to the upper limit.

Given its high packing density, it was expected that the binder composed of cement, slag 5, and limestone 4.5 would exhibit the lowest viscosity and yield stress values. However, this binder exhibited the highest viscosity and yield stress values. In fact, the packing density of particles is not the only parameter to be considered in optimizing the rheology of a suspension; particle size is also a crucial parameter that should be taken into account.

The suspensions with the highest and the lowest rheological parameters were used to investigate the effect of physical optimization on the workability and strength development of mortar mixtures. The mortar mixtures were proportioned with a constant content of standard sand. In addition, a third mortar was also proportioned using the optimized binder with a modified composition (50% cement, 30% slag 5, and 20% limestone 11.5). The rheological properties of the investigated paste and mortar mixtures are summarized in Table 6. On the other hand, the seven-day and 28-day compressive strength of the investigated mortar mixtures are presented in Figure 5.

**Table 6. Rheological properties of cement pastes and mortars**

| Mortar | E/P | Paste | | Mortar | | |
|---|---|---|---|---|---|---|
| | | Plastic viscosity of non-plasticized paste | Yield stress of non-plasticized paste | Spread (mm) | Viscosity (Pa.s) | Yield stress (Pa) |
| **M1-S5L4.5** | 0.45 | 0.6 | 17.5 | 180 | 4.2 | 64 |
| **M2-S5L11.5** | 0.45 | 0.5 | 12 | 220 | 1.7 | 17 |
| **M3-S5L11.5** | 0.36 | 1.7* | 29* | 175 | 4.7 | 77 |

*calculated

According to Table 6, the rheological parameters of mortar mixtures follow the same trend as those of their corresponding paste matrices, as expressed in Eqs. 16 and 17 [43-45].

$$\mu_{mortar} = \mu_{paste} * f\left(\phi, \phi_{max}, V_p, V_s, \mathfrak{y}\right) \quad (16)$$

$$\tau_{mortar} = \tau_{paste} * g\left(\phi, \phi_{max}, V_p, V_s, \mathfrak{y}\right) \quad (17)$$

where $\phi$ is the solid volume fraction in mortar, $\phi_{max}$ is the maximum packing density of sand, $V_P$ is the paste volume, $V_S$ is the sand volume, and $\mathfrak{y}$ is the intrinsic viscosity.

The impact of the physical optimization of cementitious powders on the rheology of mortar mixtures was investigated. Given that the mortars M1-S5L4.5 and M2 -S5L11.5 have the same solid fraction, and that they were both proportioned using PCE, it can be noted based on (eq.16) that $\frac{\tau_{0-\text{M2}-\text{S5L11.5}}}{\tau_{0-\text{M1}-\text{S5L4.5}}} = \frac{\tau_{0-\text{paste}-\text{S5L11.5}-\text{pce}}}{\tau_{0-\text{paste}-\text{S5L4.5}-\text{pce}}} = 30\%$ , whereas the experimental rheological results obtained using the non-superplasticized cement paste provided a ratio of $\frac{\tau_{0-\text{paste}-\text{S5L11.5}}}{\tau_{0-\text{paste}-\text{S5L4.5}}} = 65\%$. This means that 35% of the noted reduction in the rheological property is related to physical optimization, while the complementary reduction of 35% is related to the presence of superplasticizers. Indeed, because the S5L4.5 powder is finer than S5L11.5 and both powders have the same chemical composition, it can be assumed that the optimized powder's (i.e. S5L11.5) need for superplasticizer is lower. A given concentration of superplasticizer resulted in greater superplasticizer surface coverage for the optimized powder, allowing a more significant decrease in the rheological properties of the paste and mortar.

As shown in Table 6, the optimized mortar M3-S5L11.5 exhibited similar rheological properties to those of the reference mortar M1- S5L4.5, while decreasing the water-to-powder ratio from 0.45 to 0.36. We recall that the optimized mortar contains less clinker powder (50% cement, 30% slag, and 20% limestone) than the reference mortar. The enhanced fluidity may be due to both physical optimization and the lower demand for superplasticizer. Indeed, for lower clinker content or larger particle sizes, the demand for superplasticizer decreases.

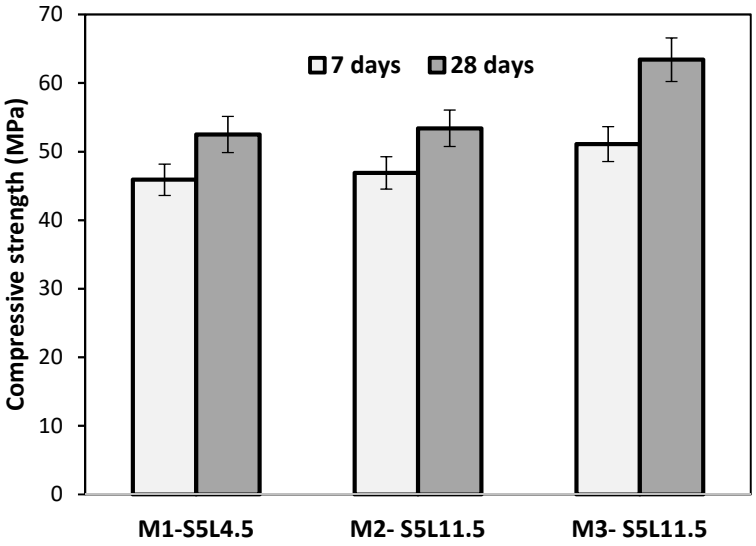


**Figure 5. 7- and 28-days compressive strength of the investigated mortar mixtures**

As shown in Figure 5, for a given age, the M1-S5L4.5 and M2-S5L11.5 mortar mixtures developed very similar compressive strength, while the M3-S5L11.5 mortar exhibited higher compressive strength, especially after 28 days of age. The mortars M1-S5L4.5 and M2-S5L11.5 were proportioned using an equal water-to-binder ratio, but M1-S5L4.5 was made with the ground powder reflecting higher fineness. The blended cement powders used in these mortars have different particle-size distributions and equal packing density. From Table 1, we note that if the two powders have the same chemistry, the mortars M1-S5L4.5 and M2-S5L11.5 should exhibit equal mechanical strength, which was confirmed by our experimental results. These results confirm the initially adopted assumption that the soft grinding of slag and limestone powders in this study did not influence the reactivity of the investigated binders. Moreover, the M2-S5L11.5 mortar is more fluid than M1-S5L4.5. As expected from Table 1, optimizing the physical characteristics of blended powders resulted in a more fluid mortar without any significant impact on its strength development.

The M3-S5L11.5 mortar showed the best compressive strength with a gain of 10 MPa after 28 days of age compared to the reference mortar (M1-S5L4.5). It is worth mentioning that the M3-mortar was made with only 50% cement, compared to 65% used in the reference mortar (M1-mortar). The improvement in compressive strength is mainly due to the lower water-to-powder ratio, which resulted in a more compact matrix. The gain in compressive strength may also be partially related to the existence of a relatively higher concentration of non-adsorbed superplasticizer in the interstitial fluid [46]. The results obtained clearly reflect

the usefulness of optimizing physical characteristics, which goes beyond just the fluidification of the paste, and can help in the design of greener cements with improved compressive strength development. As shown in Figure 5, the optimized ternary binder is more resistant even though it contains less clinker, and is less costly because the inert materials are less ground, while achieving comparable fluidity level with the reference mixture

# 5. Conclusion

A methodology was proposed to enhance the rheological properties of blended cement suspensions through the optimization of the physical characteristics of the binders. A reference cement-slag-limestone ternary cement was used to help assess the advantages of optimizing the physical characteristics of single powders and fillers to achieve suspensions with higher fluidity. The most promising physical characteristics to optimize in the case of non-plasticized suspensions are particle-size distribution and the maximum packing density of powders. These characteristics were successfully estimated for blended cements using existing models. Their effects on rheology of suspensions were highlighted. This approach allowed the selection of powders with the physical characteristics required to enhance the rheology of suspension. Finally, the study showed that optimizing the physical characteristics of blended binders with constant chemical composition improved strength development, regardless of the age of mortar mixtures, while keeping the same level of fluidity. In the case of 28-day compressive strength, a 20% gain was obtained with a lower clinker content (50% vs. 65%).

**Appendix A: The viscosity model**

A recent study made it possible to suggest a predictive model of the viscosity of cementitious suspensions for single mineral powders based on the physical characteristics of the powder, the solid volume fraction in the paste, and the viscosity of the interstitial fluid [27]. The equation is given by:

$$\mu = \alpha\, \mu_0 \frac{a^{*2}}{h d_{50}} \left(1 - \frac{\phi}{\phi_{max}}\right)^{-\beta} \quad \text{(A.1)}$$

While keeping the same notations defined in the above, d is the volume mean diameter, and $\alpha$ and β are fitting parameters.

In [27] the mean radius curvature of mineral powders was estimated from the yield stress measurements and the Yodel [14]. In Figure A-1 we plot the obtained particle roughness of mineral powders from [27]. The particle roughness for the five studied mineral powders with different particle sizes (clinker, slag, four limestones, five quartzes, and fly ash) is very similar and is estimated to be around 800 nm. Using experimental results from [27], we plot the relative residual viscosity multiplied by $\frac{d}{a^{*2}}h$ as a function of the relative solid volume fraction in

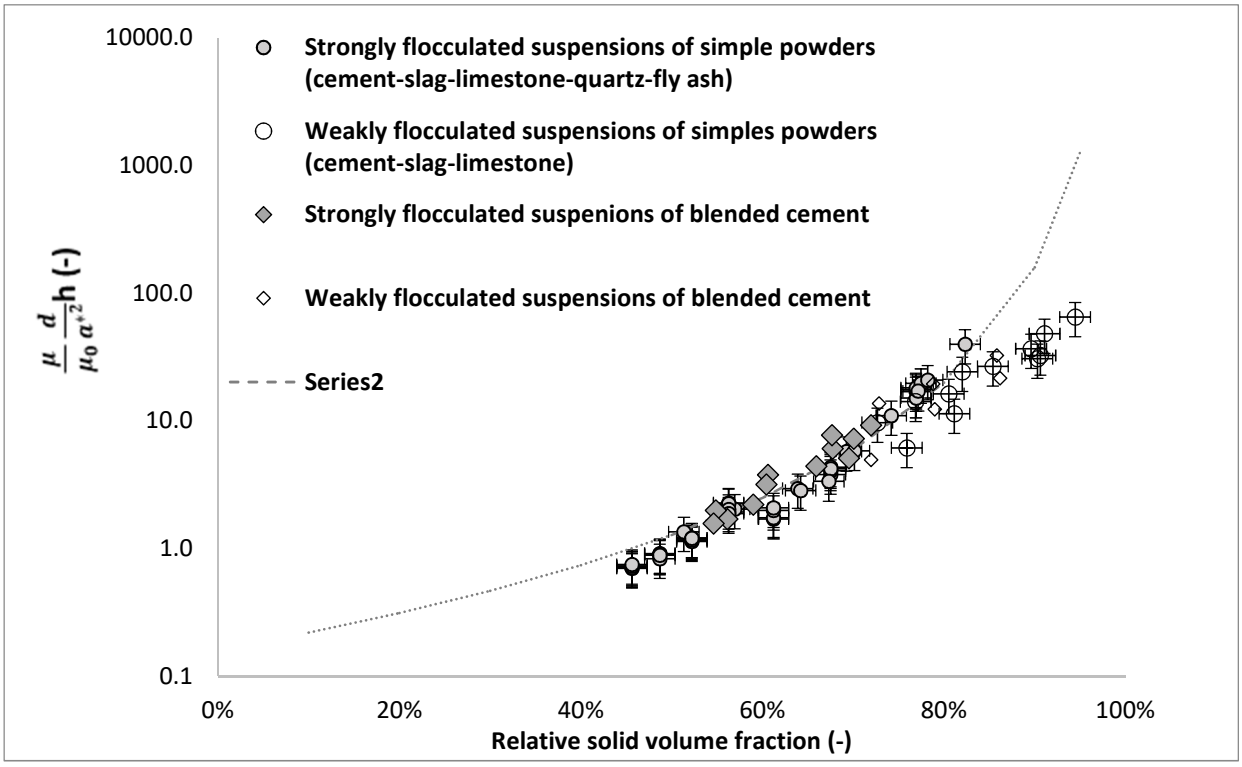


Figure **A-**2. The values of roughness are from Figure A-1. The results provide a master curve gathering all strongly flocculated (i.e. without plasticizers) and weakly flocculated suspensions (i.e. with plasticizers) of rough cementitious powders (cement, slag, limestone, quartz, and fly ash) corroborating the scaling established in Eq. (A.1), with $\alpha = 0.16$ and $\beta = 3$ .

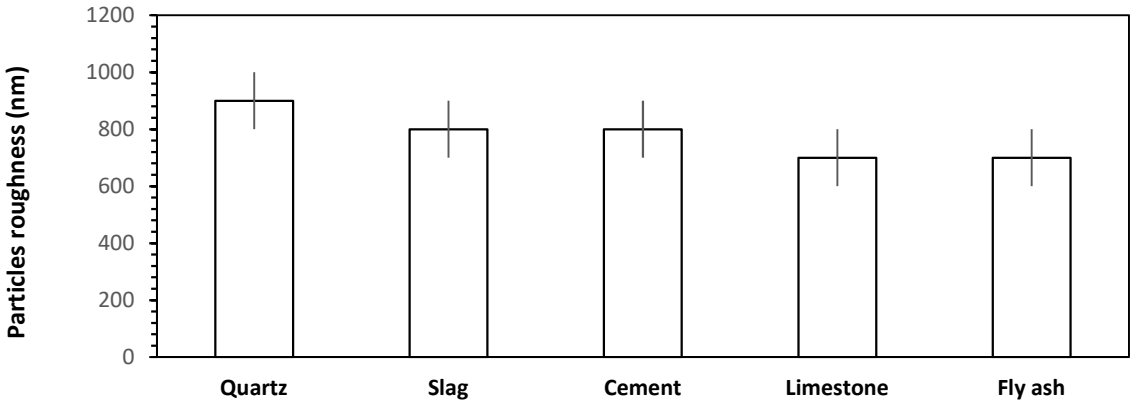


**Figure A-1. Computed values of mean radius of curvature for cement, slag, limestone, fly ash, and quartz** *[27]*

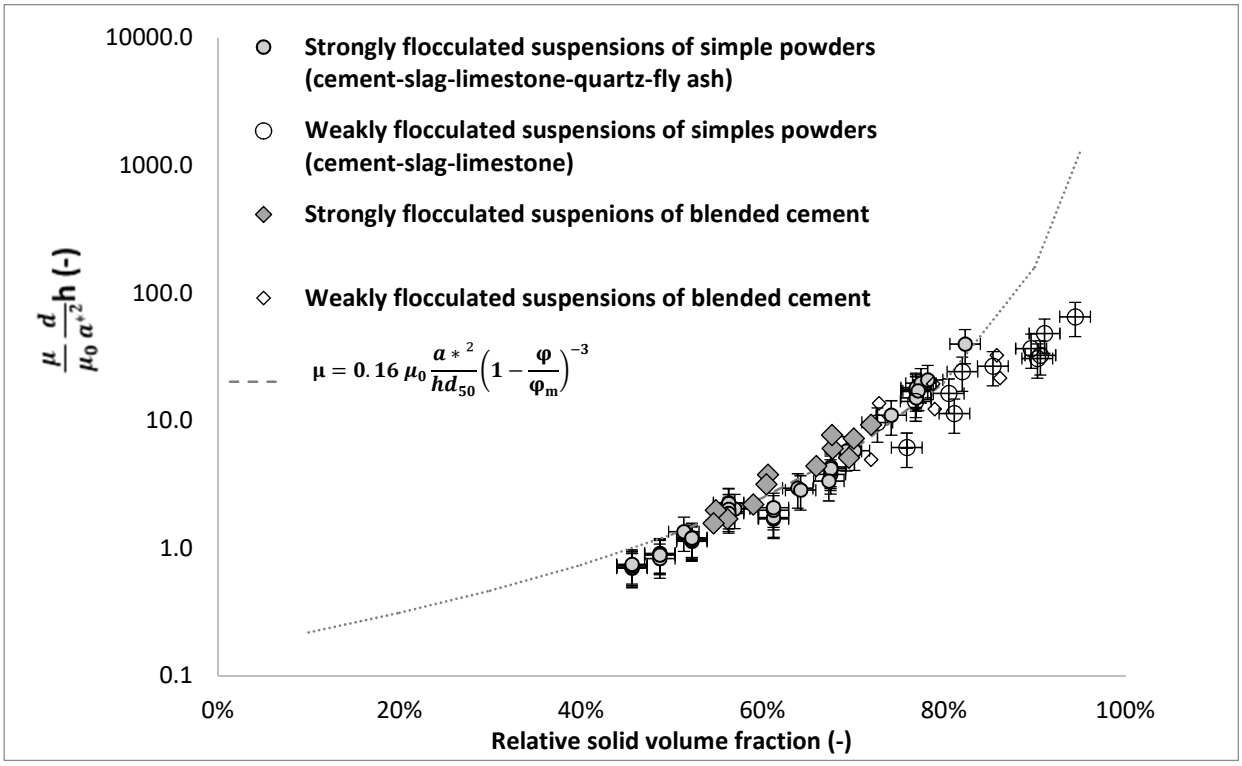


**Figure A-2. Relative residual viscosity multiplied by $\frac{d_{50}}{a^{*2}} h$ as a function of the relative solid volume fraction for flocculated suspensions. Adapted from [27]**

## Appendix B: Yield stress calculation using the Yodel.

We recall the Yodel model given by [14]:

$$\tau = m_1 \frac{\emptyset(\emptyset - \emptyset_0)^2}{\emptyset_{max}(\emptyset_{max} - \emptyset)} \qquad m_1 = \frac{0.15 * \mu_{k,k} A_0 a^*}{\pi^4 h^2} \frac{f^*_{\sigma,\Delta}}{R^2_{v,50}} \qquad (1)$$

Considering results from Figure A-1, we assume that the surface roughness a*, which is the mean radius of curvature at contact points, is almost the same for all the powders and is of the order of 800 nm.

The solid volume fraction of the suspensions was calculated for a water-to-powder ratio of 0.45 by mass. Table B-1 shows the different values of the parameters used for the calculation of the yield stress and the plastic viscosity. The undelayed Hamaker constant $A_0$ was calculated by averaging the Hamaker constants of each cement, slag, and limestone according to the percentage of each of the powders. Given the error in the measurement of the particle-size distributions, it was assumed that all particle-size distributions have a similar shape and that $f_{\sigma,\Delta}^{*}$ is of the order of 2.

**Table B-1. Parameter used to calculate yield stress and viscosity of ternary cement suspensions**

| **Parameter** | $A_0$ | **h** | **a*** | $f_{\sigma,\Delta}^{*}$ | $\phi_{perc}$ |
|---|---|---|---|---|---|
| **Used value** | 1,61E-20 | 1.6 nm | 800 nm | 1.9 | 20% |

**Appendix C: Slag Datasheets**

**Slag 8.5** **Slag 5.5**

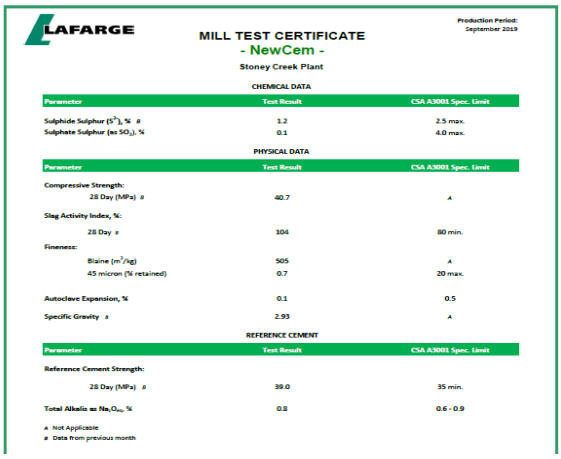

LAFARGE

MILL TEST CERTIFICATE
- NewCem -
Stoney Creek Plant

Production Period: September 2019

CHEMICAL DATA

| Parameter | Test Result | CSA A3001 Spec. Limit |
|---|---|---|
| Sulphide Sulphur ($S^{2-}$), % # | 1.2 | 2.5 max. |
| Sulphate Sulphur (as $SO_3$), % | 0.1 | 4.0 max. |

PHYSICAL DATA

| Parameter | Test Result | CSA A3001 Spec. Limit |
|---|---|---|
| Compressive Strength: | | |
| 28 Day (MPa) # | 40.7 | A |
| Slag Activity Index, %: | | |
| 28 Day # | 104 | 80 min. |
| Fineness: | | |
| Blaine ($m^2$/kg) | 505 | A |
| 45 micron (% retained) | 0.7 | 20 max. |
| Autoclave Expansion, % | 0.1 | 0.5 |
| Specific Gravity # | 2.93 | A |

REFERENCE CEMENT

| Parameter | Test Result | CSA A3001 Spec. Limit |
|---|---|---|
| Reference Cement Strength: | | |
| 28 Day (MPa) # | 39.0 | 35 min. |
| Total Alkalis as $Na_2O_{eq}$, % | 0.8 | 0.6 - 0.9 |

A Not Applicable
# Data from previous month

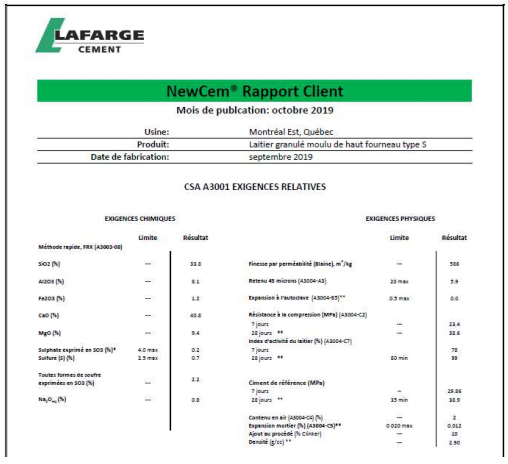

LAFARGE CEMENT

NewCem® Rapport Client

Mois de publcation: octobre 2019

| | |
|---|---|
| Usine: | Montréal Est, Québec |
| Produit: | Laitier granulé moulu de haut fourneau type S |
| Date de fabrication: | septembre 2019 |

CSA A3001 EXIGENCES RELATIVES

EXIGENCES CHIMIQUES

| | Limite | Résultat |
|---|---|---|
| Méthode rapide, FRX (A3063-08) | | |
| SiO2 (%) | --- | 33.0 |
| Al2O3 (%) | --- | 8.1 |
| Fe2O3 (%) | --- | 1.2 |
| CaO (%) | --- | 40.8 |
| MgO (%) | --- | 9.4 |
| Sulphate exprimé en SO3 (%)* | 4.0 max | 0.2 |
| Sulfure (S) (%) | 2.5 max | 0.7 |
| Toutes formes de soufre exprimées en SO3 (%) | --- | 2.2 |
| $Na_2O_{eq}$ (%) | --- | 0.8 |

EXIGENCES PHYSIQUES

| | Limite | Résultat |
|---|---|---|
| Finesse par perméabilité (Blaine), $m^2$/kg | --- | 506 |
| Refus 45 microns (A3004-A3) | 20 max | 5.9 |
| Expansion à l'autoclave (A3004-B3)** | 0.5 max | 0.0 |
| Résistance à la compression (MPa) (A3004-C2) | | |
| 7 jours | --- | 23.4 |
| 28 jours ** | --- | 36.6 |
| Indice d'activité du laitier (%) (A3004-C7) | | |
| 7 jours | | 78 |
| 28 jours ** | 80 min | 99 |
| Ciment de référence (MPa) | | |
| 7 jours | -- | 28.86 |
| 28 jours ** | 35 min | 38.9 |
| Contenu en air (A3004-C6) (%) | --- | 2 |
| Expansion mortier (%) (A3004-C5)** | 0.020 max | 0.012 |
| Ajout au procédé (% Clinker) | --- | 10 |
| Densité (g/cc) ** | --- | 2.90 |

## Slag 6.5

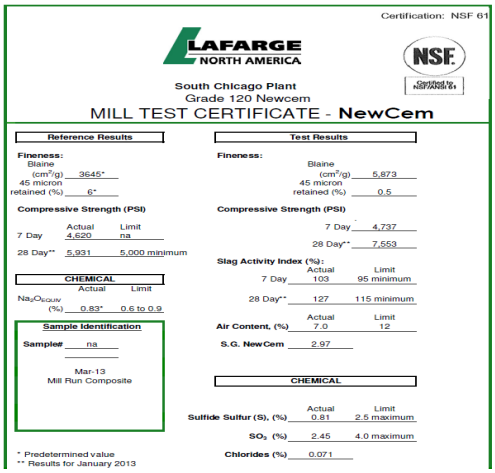

Certification: NSF 61

LAFARGE NORTH AMERICA

NSF Certified to NSF/ANSI/CAN 61

South Chicago Plant
Grade 120 Newcem
MILL TEST CERTIFICATE - NewCem

**Reference Results**

Fineness:
Blaine ($cm^2$/g) 3645*
45 micron retained (%) 6*

Compressive Strength (PSI)

| | Actual | Limit |
|---|---|---|
| 7 Day | 4,620 | na |
| 28 Day** | 5,931 | 5,000 minimum |

CHEMICAL

| | Actual | Limit |
|---|---|---|
| $Na_2O_{equiv}$ (%) | 0.83* | 0.6 to 0.9 |

Sample Identification
Sample# na
Mar-13
Mill Run Composite

* Predetermined value
** Results for January 2013

**Test Results**

Fineness:
Blaine ($cm^2$/g) 5,873
45 micron retained (%) 0.5

Compressive Strength (PSI)
7 Day 4,737
28 Day** 7,553

Slag Activity Index (%):

| | Actual | Limit |
|---|---|---|
| 7 Day | 103 | 95 minimum |
| 28 Day** | 127 | 115 minimum |

| | Actual | Limit |
|---|---|---|
| Air Content, (%) | 7.0 | 12 |

S.G. NewCem 2.97

CHEMICAL

| | Actual | Limit |
|---|---|---|
| Sulfide Sulfur (S), (%) | 0.81 | 2.5 maximum |
| $SO_3$ (%) | 2.45 | 4.0 maximum |
| Chlorides (%) | 0.071 | |

# References


[1] KNOP, Yaniv, PELED, Alva, et COHEN, Ronen. Influences of limestone particle size distributions and contents on blended cement properties. *Construction and Building Materials*, 2014, vol. 71, p. 26-34.

[2] Aıtcin PC (1998) High performance concrete. E&FN Spon, London

[3] ZHANG, Chengzhi, WANG, Aiqin, TANG, Mingshu, *et al.* The filling role of pozzolanic material. *Cement and Concrete Research*, 1996, vol. 26, no 6, p. 943-947.

[4] FERRARIS, Chiara F., OBLA, Karthik H., et HILL, Russell. The influence of mineral admixtures on the rheology of cement paste and concrete. *Cement and concrete research*, 2001, vol. 31, no 2, p. 245-255.

[5] WONG, H. H. C., NG, I. Y. T., NG, P. L., *et al.* Increasing packing density through blending cement, fly ash and silica fume to improve cement paste rheology. In : *ACI Special Publication SP-242-17, 9th CANMET/ACI International Conference on Fly Ash, Silica Fume, Slag and Natural Pozzolans in Concrete in Warsaw, Poland*. 2007. p. 221-225.

[6] Jared E. Brewe, John J. Myers, PARTICLE SIZE OPTIMIZATION FOR REDUCED CEMENT HIGH STRENGTH CONCRETE, 2005 NBC

[7] KWAN, A. K. H. et WONG, H. H. C. Effects of packing density, excess water and solid surface area on flowability of cement paste. *Advances in Cement Research*, 2008, vol. 20, no 1, p. 1-11.

[8] LEE, Seung Heun, KIM, Hong Joo, SAKAI, Etsuo, *et al.* Effect of particle size distribution of fly ash–cement system on the fluidity of cement pastes. *Cement and Concrete Research*, 2003, vol. 33, no 5, p. 763-768.

[9] DAMINELI, Bruno L., JOHN, Vanderley M., LAGERBLAD, Björn, *et al.* Viscosity prediction of cement-filler suspensions using interference model: A route for binder efficiency enhancement. *Cement and Concrete Research*, 2016, vol. 84, p. 8-19.

[10] JOHN, Vanderley M., DAMINELI, Bruno L., QUATTRONE, Marco, *et al.* Fillers in cementitious materials—Experience, recent advances and future potential. *Cement and Concrete Research*, 2018, vol. 114, p. 65-78.

[11] LEE, Seung Heun, KIM, Hong Joo, SAKAI, Etsuo, *et al.* Effect of particle size distribution of fly ash–cement system on the fluidity of cement pastes. *Cement and Concrete Research*, 2003, vol. 33, no 5, p. 763-768.

[12] VANCE, Kirk, KUMAR, Aditya, SANT, Gaurav, *et al.* The rheological properties of ternary binders containing Portland cement, limestone, and metakaolin or fly ash. *Cement and Concrete Research*, 2013, vol. 52, p. 196-207.

[13] BENTZ, Dale P., FERRARIS, Chiara F., GALLER, Michael A., *et al.* Influence of particle size distributions on yield stress and viscosity of cement–fly ash pastes. *Cement and Concrete Research*, 2012, vol. 42, no 2, p. 404-409.

[14] FLATT, Robert J. et BOWEN, Paul. Yodel: a yield stress model for suspensions. *Journal of the American Ceramic Society*, 2006, vol. 89, no 4, p. 1244-1256.

[15] YOUNESS, Dima, HOSSEINPOOR, Masoud, YAHIA, Ammar, *et al.* Flowability characteristics of dry supplementary cementitious materials using Carr measurements and their effect on the rheology of suspensions. *Powder Technology*, vol. 378, p. 124-144.

[16] YOUNESS, Dima, YAHIA, Ammar, et TAGNIT-HAMOU, Arezki. Coupled rheo-physical effects of blended cementitious materials on wet packing and flow properties of inert suspensions. *Construction and Building Materials*, 2020, p. 121588. (accepted, October 2020).

[17] FLATT, Robert J. et BOWEN, Paul. Yield stress of multimodal powder suspensions: an extension of the YODEL (Yield Stress mODEL). *Journal of the American Ceramic Society*, 2007, vol. 90, no 4, p. 1038-1044.

[18] ROUSSEL, Nicolas, LEMAÎTRE, Anael, FLATT, Robert J., *et al.* Steady state flow of cement suspensions: A micromechanical state of the art. *Cement and Concrete Research*, 2010, vol. 40, no 1, p. 77-84.

[19] FLATT, R.J. Chap. 7 — Superplasticizers and the rheology of concrete, in: N. Roussel (Ed.), Understanding the Rheology of Concrete, Woodhead Publishing, 2012, pp. 144–208.

[20] HOT, Julie, BESSAIES-BEY, Hela, BRUMAUD, Coralie, et al. Adsorbing polymers and viscosity of cement pastes. *Cement and Concrete Research*, 2014, vol. 63, p. 12-19.

[21] MARCHON, Delphine, KAWASHIMA, Shiho, BESSAIES-BEY, Hela, *et al.* Hydration and rheology control of concrete for digital fabrication: Potential admixtures and cement chemistry. *Cement and Concrete Research*, 2018, vol. 112, p. 96-110.

[22] LEWIS, Jennifer A., MATSUYAMA, Hiro, KIRBY, Glen, *et al.* Polyelectrolyte effects on the rheological properties of concentrated cement suspensions. *Journal of the American Ceramic Society*, 2000, vol. 83, no 8, p. 1905-1913.

[23] FLATT, Robert J. et HOUST, Yves F. A simplified view on chemical effects perturbing the action of superplasticizers. *Cement and Concrete Research*, 2001, vol. 31, no 8, p. 1169-1176.

[24] LAI, Guangxing, FANG, Yunhui, CHEN, Zhanghua, *et al.* Effect of cement particle size distribution on properties of cement mixed with polycarboxylate superplasticizer. In: *IOP Conference Series: Materials Science and Engineering*. IOP Publishing, 2020. p. 042013.

[25] ARORA, Aashay, AGUAYO, Matthew, HANSEN, Hannah, *et al.* Microstructural packing-and rheology-based binder selection and characterization for Ultra-High-Performance Concrete (UHPC). *Cement and Concrete Research*, 2018, vol. 103, p. 179-190.

[26] SEDRAN, Thierry RHEOLOGIE ET RHEOMETRIE DES BETONS. APPLICATION AUX BETONS AUTONIVELANTS, 1999

[27] AHMADAH, Oumayma, Contrôle de la rhéologie des liants à faibles impacts environnementaux, Université de Paris-est, Université de Sherbrooke, 2021

[28] GELARDI, G., and FLATT, R.J. "Working mechanisms of water reducers and superplasticizers." *Science and Technology of Concrete Admixtures*. Woodhead Publishing, 2016. 257-278.

[29] PERROT, Arnaud, LECOMPTE, Thibaut, KHELIFI, Hamid, *et al.* Yield stress and bleeding of fresh cement pastes. *Cement and Concrete Research*, 2012, vol. 42, no 7, p. 937-944.

[30] UKRAINCZYK, Neven, THIEDEITZ, Mareike, KRÄNKEL, Thomas, *et al.* Modeling SAOS Yield Stress of Cement Suspensions: Microstructure-Based Computational Approach. *Materials*, 2020, vol. 13, no 12, p. 2769.

[31] BENTZ, Dale P., GARBOCZI, Edward J., HAECKER, Claus J., *et al.* Effects of cement particle size distribution on performance properties of Portland cement-based materials. *Cement and Concrete Research*, 1999, vol. 29, no 10, p. 1663-1671.

[32] POMMERSHEIM, James M. Effect of particle size distribution on hydration kinetics. *MRS Online Proceedings Library Archive*, 1986, vol. 85.

[33] CELIK, I. B. The effects of particle size distribution and surface area upon cement strength development. *Powder Technology*, 2009, vol. 188, no 3, p. 272-276.

[34] BENTZ, Dale P. et HAECKER, Claus J. An argument for using coarse cements in high-performance concretes. *Cement and concrete research*, 1999, vol. 29, no 4, p. 615-618.

[35] ZHOU, Zhongwu, SOLOMON, Michael J., SCALES, Peter J., *et al.* The yield stress of concentrated flocculated suspensions of size distributed particles. *Journal of Rheology*, 1999, vol. 43, no 3, p. 651-671.

[36] GONG, Jianqing, CHOU, Kai, HUANG, Zheng Yu, *et al.* A quantitative study on packing density and pozzolanic activity of cementitious materials based on the compaction packing model. In : *IOP Conference Series: Materials Science and Engineering*. IOP Publishing, 2014. p. 012013.

[37] WEBB, Paul A. Volume and density determinations for particle technologists. *Micromeritics Instrument Corp*, 2001, vol. 2, no 16, p. 01.

[38] CONCRETE, Fresh. Compactibility With IC–Tester–Method NT BUILD 427. *Nordtest Scandinavian Institution*, 1994.

[39] SEDRAN, Thierry, DE LARRARD, François, et LE GUEN, Laurédan. Détermination de la compacité des ciments et additions minérales à la sonde de Vicat. 2007

[40] ASTM, C. Standard practice for mechanical mixing of hydraulic cement pastes and mortars of plastic consistency. *ASTM West Conshohocken, PA*, 2014.

[41] ROUSSEL, Nicolas, Understanding the Rheology of Concrete, chap 4, 2012

[42] HOSSEINPOOR, Masoud, KOURA, Baba-Issa Ouro, YAHIA, Ammar, *et al.* Diphasic investigation of the visco-elastoplastic characteristics of highly flowable fine mortars. *Construction and Building Materials*, 2020, p. 121425.

[43] KRIEGER, Irvin M. et DOUGHERTY, Thomas J. A mechanism for non-Newtonian flow in suspensions of rigid spheres. *Transactions of the Society of Rheology*, 1959, vol. 3, no 1, p. 137-152.

[44] CHATEAU, Xavier, OVARLEZ, Guillaume, et TRUNG, Kien Luu. Homogenization approach to the behavior of suspensions of noncolloidal particles in yield stress fluids. *Journal of Rheology*, 2008, vol. 52, no 2, p. 489-506.

[45] KABAGIRE, K. Daddy, DIEDERICH, Paco, YAHIA, Ammar, *et al.* Experimental assessment of the effect of particle characteristics on rheological properties of model mortar. *Construction and Building Materials*, 2017, vol. 151, p. 615-624.

[46] FERNÁNDEZ, José María, DURAN, Adrián, NAVARRO-BLASCO, I., *et al.* Influence of nanosilica and a polycarboxylate ether superplasticizer on the performance of lime mortars. *Cement and Concrete Research*, 2013, vol. 43, p. 12-24.